

# Absolute Magnitude Calibration for Red Clump Stars

S. Karaali<sup>1</sup> • S. Bilir<sup>1</sup> • E. Yaz Gökçe<sup>1</sup>

**Abstract** We combined the ( $K_s$ ,  $V - K_s$ ) data in Laney et al. (2012) with the  $V$  apparent magnitudes and trigonometric parallaxes taken from the *Hipparcos* catalogue and used them to fit the  $M_{K_s}$  absolute magnitude to a linear polynomial in terms of  $V - K_s$  colour. The mean and standard deviation of the absolute magnitude residuals,  $-0.001$  and  $0.195$  mag, respectively, estimated for 224 red clump stars in Laney et al. (2012) are (absolutely) smaller than the corresponding ones estimated by the procedure which adopts a mean  $M_{K_s} = -1.613$  mag absolute magnitude for all red clump stars,  $-0.053$  and  $0.218$  mag, respectively. The statistics estimated by applying the linear equation to the data of 282 red clump stars in Alves (2000) are larger,  $\Delta M_{K_s} = 0.209$  and  $\sigma = 0.524$  mag, which can be explained by a different absolute magnitude trend, i.e. condensation along a horizontal distribution.

**Keywords** Stars: distances, Stars: late-type, Galaxy: Solar neighbourhood

## 1 Introduction

Red Clump (RC) stars are core helium-burning giants. It is a prominent feature in the colour-magnitude diagrams of open clusters as well as globular clusters. Now,

---

S. Karaali

<sup>1</sup>Istanbul University, Faculty of Science, Department of Astronomy and Space Sciences, 34119 University, Istanbul, Turkey

S. Bilir

<sup>1</sup>Istanbul University, Faculty of Science, Department of Astronomy and Space Sciences, 34119 University, Istanbul, Turkey

E. Yaz Gökçe

<sup>1</sup>Istanbul University, Faculty of Science, Department of Astronomy and Space Sciences, 34119 University, Istanbul, Turkey

it is known that they are abundant in the solar neighbourhood. This sample of RC stars provides accurate absolute magnitude estimation due to their parallaxes which can be used in testing their suitability for a distance indicator. A mean absolute magnitude in any band with small scattering can work for the purpose of the researchers. Many works have been carried out for optical and near infrared bands such as  $V$ ,  $I$  and  $K_s$ . Their absolute magnitudes in the optical range lie from  $M_V = +0.7$  mag for those of spectral type G8 III to  $M_V = +1$  mag for type K2 III (Keenan & Barnbaum 1999). The absolute magnitude of these stars in the  $K$  band is  $M_{K_s} = -1.61 \pm 0.03$  mag with negligible dependence on metallicity (Alves 2000), but with real dispersion. Grocholski & Sarajedini (2002) claimed an absolute magnitude for the RC stars rather close to the one just cited here, with some limitations however. Based on 14 open clusters, they draw the conclusion that for clusters having  $-0.5 < [Fe/H] \leq 0$  dex and  $1.58 \leq t \leq 7.94$  Gyr, one can use  $\langle M_{K_s} \rangle = -1.61 \pm 0.04$  mag.

The dependence of the  $I$ -band magnitude on the RC stars was extensively studied in the past from an observational point of view. In most cases the  $M_I$  mean absolute magnitude is insensitive to age and metallicity (Udalski 1998). However, a modest variation in  $M_I$  with colour and metallicity has been claimed in the literature (Paczynski & Stanek 1998; Stanek & Garnavich 1998; Sarajedini 1999; Zhao et al. 2001; Kubiak et al. 2002). Theoretical models from Girardi & Salaris (2001) also show a dependence of metallicity and age in  $I$  band. Salaris & Girardi (2002) stated in their study based on the models of Girardi et al. (2000) that  $M_K$  is a complicated function of metallicity and age.

In a recent work, van der Heijden & Groenewegen (2007) used the Two Micron All Sky Survey (2MASS; Skrutskie et al. 2006) infrared data for a sample of 24 open clusters to investigate how the  $K_s$ -band ab-

solute magnitude of the red clump depends on age and metallicity. They showed that a constant value of  $M_{K_s} = -1.57 \pm 0.05$  mag is a reasonable assumption to use in distance determinations for clusters with metallicity between  $-0.5$  and  $+0.4$  dex and age between  $0.31$  and  $7.94$  Gyr. Following this work, Groenewegen (2008) claimed two absolute values in different bands for the RC stars, i.e.  $M_{K_s} = -1.54 \pm 0.04$  and  $M_I = -0.22 \pm 0.03$  mag, where the estimations were based on newly reduced the *Hipparcos* catalogue van Leeuwen (2007).

In a more recent work, Laney et al. (2012) determined the mean  $M_K$  absolute magnitude for RC stars in the solar neighbourhood to within 2 per cent ( $M_K = -1.613 \pm 0.015$  mag) and applied their results to the estimation of the distance of the Large Magellanic Cloud. A mean value for the  $M_K$  absolute magnitude with weak or negligible dependence on metallicity makes possible to use this population as a tracer of Galactic structure and interstellar extinction, as several works have fully demonstrated in the last decade (see for example Lopez-Corredoira et al. 2002, 2004; Cabrera-Lavers et al. 2005, 2007a,b, 2008; Bilir et al. 2012, and references therein).

In Bilir et al. (2013) the  $M_V$ ,  $M_J$ ,  $M_{K_s}$  and  $M_g$  absolute magnitudes of RC stars, identified by a set of constraints in the *Hipparcos* catalogue, were calibrated in terms of colour with  $BVI$ ,  $JHK_s$  and  $gri$  photometries. In the present paper, we will focus on a single absolute magnitude,  $M_{K_s}$ , which is the most probable candidate for adopting as a distance indicator. Our aim is to calibrate the  $M_{K_s}$  absolute magnitude as a function of colour. Thus, we expect more accurate absolute magnitudes relative to the procedure which adopts  $M_{K_s}$  absolute magnitude as a constant value. The procedure is given in Section 2. The data and the relation between the colour and absolute magnitude are presented in Sections 3 and 4, respectively. The application of the procedure is devoted to Section 5, and finally a discussion is given in Section 6.

## 2 The Procedure

The absolute magnitude of a star is a function of luminosity class, temperature or colour, age and metallicity. As it is assumed that the RC stars are at the same evolutionary stage, all the RC stars are of the same luminosity class. Hence, we omit this parameter in the absolute magnitude estimation of the RC stars. Many studies are based on the *Hipparcos* catalogue (van Leeuwen 2007) which involves the solar neighbourhood stars. Using the *Hipparcos* catalogue is

a constraint both in metallicity and age for the sample stars. This is the reason that the researchers claim weak dependence of the  $M_{K_s}$  absolute magnitude on age and metallicity. The advantage of the up-dated *Hipparcos* catalogue (van Leeuwen 2007) is that the errors are smaller than the former edition. The data of open clusters are also age and metallicity constraint. For example the age and metallicity intervals for 24 open clusters in van der Helshoect & Groenewegen (2007) are  $0.31 \leq t \leq 7.94$  Gyr, and  $-0.5 \leq [Fe/H] \leq +0.4$  dex, respectively. However, one can include the metal-poor globular clusters such as NGC 1261 with metallicity  $[Fe/H] = -1.35$  dex into the sample used for  $M_{K_s}$  absolute magnitude estimation of the RC stars. In this case, one expect metallicity- and age-dependent  $M_{K_s}$  absolute magnitudes. Despite age and metallicity limitations for the data used for the  $M_{K_s}$  absolute magnitude estimation, the range of the corresponding colour is large enough for considering in the estimation of the absolute magnitude in question. For example, the range of the  $V - K_s$  colour of the data used in Alves (2000) and Laney et al. (2012) is  $2 < V - K_s < 3$  mag. Then, one should consider the  $V - K_s$  colour in the  $M_{K_s}$  absolute magnitude estimation. That is, we expect more accurate  $M_{K_s}$  absolute magnitudes for individual RC stars rather than a constant value for the whole sample.

## 3 Data

We used the data of Laney et al. (2012) for calibration of the  $M_{K_s}$  absolute magnitude in terms of  $V - K_s$  colour. There are 224 RC stars in the catalogue of Laney et al. (2012). We provided the *Hipparcos* number, parallax, metallicity,  $K_s$  magnitude, and  $M_{K_s}$  absolute magnitude from the electronic version of the paper, and we added the  $V$  magnitude to this catalogue to obtain the  $V - K_s$  colours instead of  $J - K_s$  ones. The  $V$  magnitudes are taken from the *Hipparcos* catalogue. The relative parallax errors lie in the interval  $0 < \sigma_\pi/\pi \leq 0.10$  and their median is 0.03. The parallaxes were corrected by Laney et al. (2012). The data are given in Table 1. The columns give: (1) Current number, (2) *Hipparcos* number, (3) the corrected parallax, (4)  $[M/H]$  metallicity, (5)  $V$  apparent magnitude, (6)  $K_s$  apparent magnitude, (7)  $V - K_s$  colour index and (8)  $M_{K_s}$  absolute magnitude. As in Laney et al. (2012), we assumed no foreground reddening. Actually, the mean colour excess of 20 RC stars with *Hipparcos* number between 671 and 7643 in the catalogue of Laney et al. (2012), estimated by the following procedure is only  $E(B - V) = 0.017$  mag. The  $E(B - V)$  colour excess of

20 RC stars have been evaluated in two steps. First, we used the maps of Schlegel, Finkbeiner & Davis (1998) and evaluated a  $E_\infty(B-V)$  colour excess for each star. Then, we reduced them using the following procedure of Bahcall & Soneira (1980):

$$A_d(b) = A_\infty(b) \left[ 1 - \exp\left(\frac{-|d \times \sin(b)|}{H}\right) \right]. \quad (1)$$

Here,  $b$  and  $d$  are the Galactic latitude and distance to the star, respectively.  $H$  is the scale height for the interstellar dust which is adopted as 125 pc (Marshall et al. 2006).  $A_\infty(b)$  and  $A_d(b)$  are the total absorptions for the model and for the distance to the star, respectively.  $A_\infty(b)$  can be evaluated by means of the following equation:

$$A_\infty(b) = 3.1 \times E_\infty(B-V). \quad (2)$$

$E_\infty(B-V)$  is the colour excess for the model taken from the Schlegel, Finkbeiner & Davis (1998). Then,  $E_d(B-V)$ , i.e. the colour excess for the corresponding star at the distance  $d$ , can be evaluated via the equation,

$$E_d(B-V) = A_d(b) / 3.1. \quad (3)$$

The colour excess  $E_d(B-V)$  and the classical colour excess  $E(B-V)$  have the same meaning. The same case is valid for the total absorption  $A_d$  and the classical absorption  $A_V$ .

The metallicities are given only for 100 RC stars. The diagram for  $M_{K_s}$  absolute magnitude versus  $V-K_s$  colour index is given in Fig. 1. Most of the stars are concentrated in the region with  $2.1 < V-K_s < 2.6$  and  $-2 < M_{K_s} < -1$  mag. However, there are about three dozen of stars beyond these limits. The extreme colours and absolute magnitudes belong to the RC stars with *Hipparcos* numbers 3781, 37901, 38211, 58697, 63608, 70306, 72471.

#### 4 Calibration of $M_{K_s}$ Absolute Magnitude to $V-K_s$ Colour

The range of the metallicity of the sample is  $-0.7 < [M/H] < 0.4$  dex. However, 80 per cent of them lie in a smaller metallicity interval, i.e.  $-0.25 \leq [M/H] \leq +0.15$  dex (Fig. 2), indicating a thin disc sample. Hence, we preferred to use the whole sample in the calibration of  $M_{K_s}$  absolute magnitude to  $V-K_s$  colour instead of separating it into different metallicity classes.

The distribution of 80 per cent of the points in Fig. 1 is almost circular, while the complete figure gives the indication of a linear distribution. Also, the large scattering and the inhomogeneous number density hinder the selection of fitting type of the  $M_{K_s}$  absolute magnitude in terms of  $V-K_s$  colour. However, we considered all the points and fitted  $M_{K_s}$  to a linear equation in terms of  $V-K_s$  as in the following (Fig. 3):

$$M_{K_s} = -0.485(\pm 0.065) \times (V - K_s) - 0.396(\pm 0.158). \quad (4)$$

We evaluated the  $M_{K_s}$  absolute magnitude residuals, i.e. the difference between the absolute magnitude estimated by using Eq. (1) and the corresponding absolute magnitude in Table 1, and compared them with another set of absolute magnitude residuals of the same stars evaluated by adopting the value  $-1.613$  mag as the  $M_{K_s}$  absolute magnitude for all RC stars. This value was claimed by Alves (2000) and Laney et al. (2012) as the mean  $M_{K_s}$  absolute magnitude for RC stars. Eq. (4) is derived without considering the small foreground reddening in Laney et al. (2012) stated in Section 3, i.e.  $E(B-V) = 0.017$  mag. If we transform this value to the colour excess  $E(V-K_s)$  by the equation  $E(V-K_s) = 2.74 \times E(B-V)$  (Karaali, Bilir & Yaz Gökçe 2013), and use it in Eq. (4) we get an absolute magnitude fainter than 0.02 mag.

The mean absolute magnitude residuals and the corresponding standard deviations for two sets are given in the third and fourth rows of Table 2. The mean of the absolute magnitude residuals evaluated by adopting the constant absolute magnitude value  $M_{K_s} = -1.613$  mag,  $\langle \Delta M_{K_s} \rangle = -0.053$ , is 53 times larger than the one evaluated by the linear equation,  $\langle \Delta M_{K_s} \rangle = -0.001$ , in our work. Also, the standard deviation corresponding to the linear equation is smaller than the other one. However, the factor of the residuals in Fig. 4 is slightly higher than unity.

#### 5 Application of the Procedure

We applied the procedure to the data in Alves (2000). The catalogue of Alves (2000) involves 284 RC stars. We replaced the recent parallaxes and  $K_s$  band magnitudes appeared in the *Hipparcos* catalogue with the old ones. The relative parallax errors lie in the interval  $0 < \sigma_\pi/\pi \leq 0.11$  and their median is 0.02. We used the following equation of Smith (1987) to correct the observed *Hipparcos* parallaxes (van Leeuwen 2007):

$$\pi_0 = \pi \left[ \frac{1}{2} + \frac{1}{2} \sqrt{1 - 16(\sigma_\pi/\pi)^2} \right], \quad (5)$$

where  $\pi$  and  $\pi_0$  are the observed and corrected parallaxes, respectively, and  $\sigma_\pi$  denotes the error of the observed parallax.  $K_s$  apparent magnitudes are not given for two stars, *Hipparcos* number: 33449, 46952. The sample is given in Table 3. The columns give (1) current number, (2) *Hipparcos* number, (3)  $\pi_0$  corrected parallax, (4) [M/H] metallicity, (5)  $V$  apparent magnitude, (6)  $K_s$  apparent magnitude, (7)  $V - K_s$  colour index, (8)  $M_{K_s}$  absolute magnitude, and (9)  $Q$  parameter which indicates the quality of the  $JHK_s$  magnitudes of a star. The quality of the RC stars are adopted from the *Hipparcos* catalogue, and the  $M_{K_s}$  absolute magnitudes are evaluated by the following equation:

$$M_{K_s} = K_s - 10 + 2.1715 \times \ln(\pi_0), \quad (6)$$

where  $\pi_0$  is the corrected parallax of the star considered. As in Alves (2000), we assumed no foreground reddening (see also Section 3). The total number of stars for which  $M_{K_s}$  absolute magnitudes could be estimated is 282.

We plotted the  $M_{K_s}$  absolute magnitudes versus  $V - K_s$  colours for these stars in Fig. 5. The distribution of the diagram is rather different than the one given for the data in Laney et al. (2012), i.e. there is a high condensation along a horizontal line and a large scattering beyond this formation. The range of the absolute magnitudes in Fig. 5 is much larger than the one in Fig. 1,  $-3.6 \leq M_{K_s} \leq -0.3$  mag.

We evaluated the absolute magnitudes of 282 RC stars using Eq. (4) and compared them with the original ones in Table 3. The mean of the residuals and the corresponding standard deviation are  $\langle \Delta M_{K_s} \rangle = 0.209$  and  $\sigma = 0.524$  mag. As in Section 4, we evaluated another set of statistics by adopting the value  $-1.613$  mag as the  $M_{K_s}$  absolute magnitude for all RC stars, i.e.  $\langle \Delta M_{K_s} \rangle = 0.133$  and  $\sigma = 0.571$  mag (Table 2, row 4). Although the standard deviation evaluated by using the linear Eq. (4) is smaller than the one evaluated for the constant absolute magnitude, the corresponding mean of the residuals is about 1.6 times larger than the one estimated via constant absolute magnitude. The distribution of the residuals estimated by means of two procedures are given in Fig. 4.

## 6 Discussion

We combined the  $(K_s, J - K_s)$  data in Laney et al. (2012) with the  $V$  apparent magnitudes and trigonometric parallaxes taken from the *Hipparcos* catalogue and used them to fit the  $M_{K_s}$  absolute magnitude to a linear relation in terms of  $V - K_s$  colour. We preferred the data in Laney et al. (2012) for absolute magnitude

calibration in terms of colour due to the high precession of the observed magnitudes. Laney et al. (2012) used 0.75m telescope at South African Astronomical Observatory and observed the brightest and nearest RC stars in the solar neighbourhood which provide accurate data.

We evaluated the  $M_{K_s}$  absolute magnitude residuals, i.e. the difference between the absolute magnitude estimated by using Eq. (4) and the corresponding absolute magnitude in Table 1, and compared them with another set of absolute magnitude residuals of the same stars evaluated by adopting the value  $-1.613$  mag as the  $M_{K_s}$  absolute magnitude for all RC stars. This value was claimed by Alves (2000) and Laney et al. (2012) as the mean  $M_{K_s}$  absolute magnitude for RC stars. The mean of the absolute magnitude residuals evaluated by adopting the constant absolute magnitude value  $M_{K_s} = -1.613$  mag,  $\langle \Delta M_{K_s} \rangle = -0.053$  mag, is 53 times larger than the one evaluated by the linear equation  $\langle \Delta M_{K_s} \rangle = -0.001$  mag in our work. Also, the standard deviation corresponding to the linear equation is smaller than the other one. This comparison shows that the  $M_{K_s}$  absolute magnitudes estimated by a linear equation in terms of colour are more accurate than the constant absolute magnitudes. The result obtained from the application of the procedure to the data in Alves (2000) is a bit different, however. Although the standard deviation corresponding to the linear equation is smaller than the one evaluated for constant absolute magnitude, the mean of the absolute magnitude residuals estimated via linear equation is 1.6 times larger than the other one. Differences between the statistics estimated for two sets of data originate from their trends of  $M_{K_s} \times (V - K_s)$  colour magnitude diagrams. The distribution of colour-magnitude diagram for the data in Laney et al. (2012) is almost diagonal, whereas the absolute magnitudes of RC stars in Alves (2000) are condensed along a horizontal line,  $M_{K_s} \sim -1.5$  mag. As one can see in the Table 3, the 2MASS data are not of best quality which probably affect the accuracy of the estimated absolute magnitudes.

**Conclusion:** It has been suggested that RC stars are standard candles and a mean value of  $M_{K_s} = -1.613$  mag based on the *Hipparcos* data has been claimed for them in the literature. In this study, we showed that the absolute magnitude for the  $K_s$  band is colour dependent. However, we need data of best quality and a large sample in order to obtain a standard linear calibration of  $M_{K_s}$  absolute magnitude in terms of colour.

## Acknowledgments

This work has been supported in part by the Scientific and Technological Research Council (TÜBİTAK)

112T120. We thank to Dr. Martin Lopez-Corredoira for his comments and suggestions. This research has made use of NASA's Astrophysics Data System and the SIMBAD database, operated at CDS, Strasbourg, France.

## References

- Alves, D. R. 2000, ApJ, 539, 732  
 Bahcall, J.N., Soneira, R.M. 1980, ApJS, 44, 73  
 Bilir, S., Karaali, S., Ak, S., Önal, Ö., Dağtekin, N. D., Yontan, T., Gilmore, G., Seabroke, G. M. 2012, MNRAS, 421, 3362  
 Bilir, S., Önal, Ö., Karaali, S., Cabrera-Lavers, A., Çakmak, H. 2013, Ap&SS, 344, 417  
 Cabrera-Lavers, A., Garzón, F., Hammersley, P. L. 2005, A&A, 433, 173  
 Cabrera-Lavers, A., Hammersley, P.L., González-Fernández, C., López-Corredoira, M., Garzón, F., Mahoney, T. J. 2007a, A&A, 465, 825  
 Cabrera-Lavers, A., Bilir, S., Ak, S., Yaz, E., López-Corredoira, M. 2007b, A&A, 464, 565  
 Cabrera-Lavers, A., González-Fernández, C., Garzón, F., Hammersley, P. L., López-Corredoira, M. 2008, A&A, 491, 781  
 Girardi, L., Bressan, A., Bertelli, G., Chiosi, C. 2000, A&AS, 141, 371  
 Girardi, L., Salaris, M. 2001, MNRAS, 323, 109  
 Grocholski, A. J., Sarajedini A. 2002, AJ, 123, 1603  
 Groenewegen, M. A. T. 2008, A&A, 488, 935  
 Karaali, S., Bilir, S., Yaz Gökçe, E. 2013, PASA, 30, 11  
 Keenan, P.C., Barnbaum, C. 1999, ApJ, 518, 859  
 Kubiak, M., McWilliam, A., Udalski, A., Gorski, K. 2002, AcA, 52, 159  
 Laney, C. D., Joner, M. D., Pietrzyński, G. 2012, MNRAS, 419, 1637  
 López-Corredoira, M., Cabrera-Lavers, A., Garzón, F., Hammersley, P. L. 2002, A&A, 394, 883  
 López-Corredoira, M., Cabrera-Lavers, A., Gerhard, O., Garzón, F. 2004, A&A, 421, 953  
 Marshall, D.J., Robin, A.C., Reylé, C., Schultheis, M., Pi-caud, S. 2006, A&A, 453, 635  
 Páczynski, B., Stanek, K. Z. 1998, ApJ, 494, L219  
 Salaris, M., Girardi, L. 2002, MNRAS, 337, 332  
 Sarajedini, A. 1999, AJ, 118, 2321  
 Schlegel, D. J., Finkbeiner, D. P., Davis, M. 1998, ApJ 500, 525  
 Skrutskie, M. F., et al. 2006, AJ, 131, 1163  
 Smith, H. Jr., 1987, A&A 171, 336  
 Stanek, K. Z., Garnavich, P. M. 1998, ApJ, 503, L131  
 Udalski, A. 1998, AcA, 48, 383  
 van der Helshoecht, V., Groenewegen, M.A.T. 2007, A&A, 463, 559  
 van Leeuwen, F. 2007, A&A, 474, 653  
 Zhao, G., Qiu, H. M., Mao, S. 2001, ApJ, 551L, 85

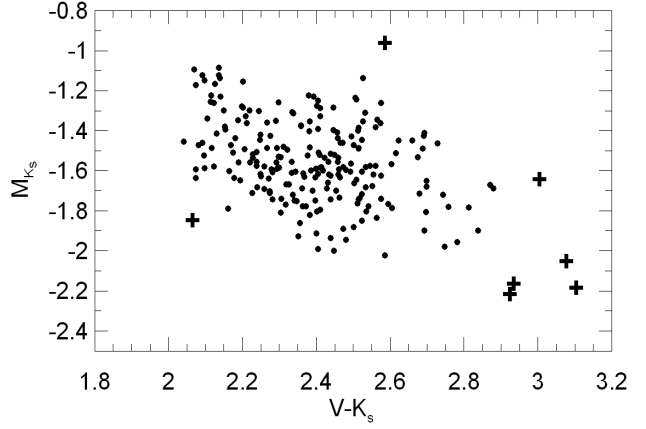


**Fig. 1**  $M_{K_s} \times (V - K_s)$  colour-absolute magnitude diagram for RC stars in Table 1. The symbol (+) indicates stars with large scattering.

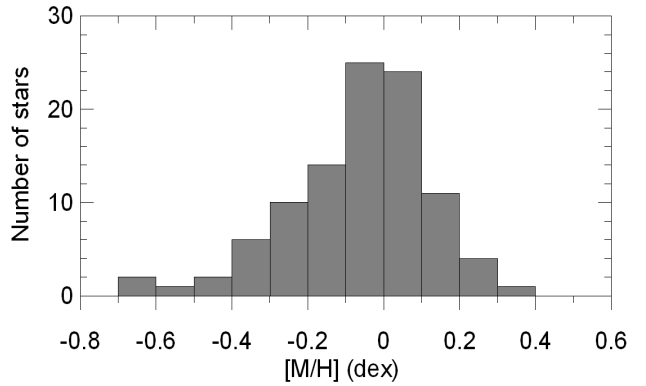


**Fig. 2** Metallicity distribution for 100 RC stars in Laney et al. (2012).

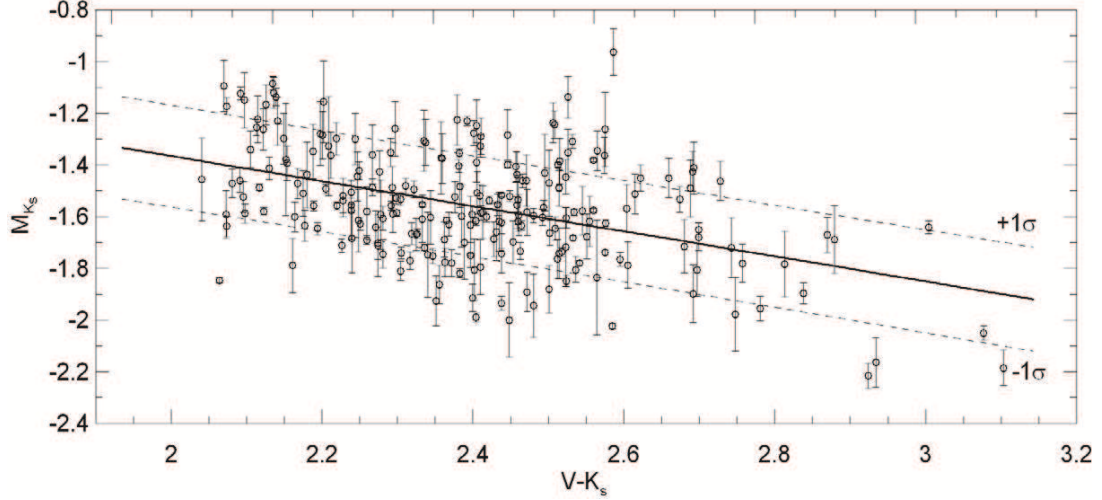


**Fig. 3** Calibration of  $M_{K_s}$  absolute magnitude in terms of  $V - K_s$ .

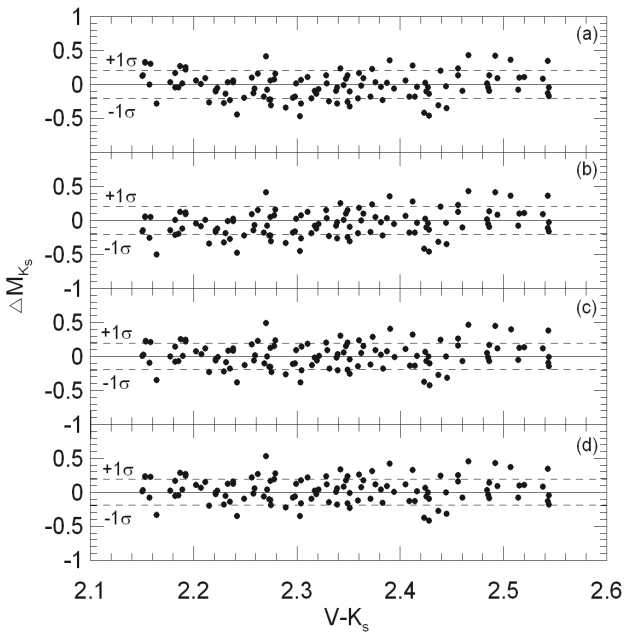


**Fig. 4** Residuals for the data in Laney et al. (2012), panels (a) and (b); and in Alves (2000), panels (c) and (d). Residuals in (a) and (c) are evaluated by the linear equation given in this study, while those in (b) and (d) correspond to the constant absolute magnitude,  $M_{K_s} = -1.613$  mag.

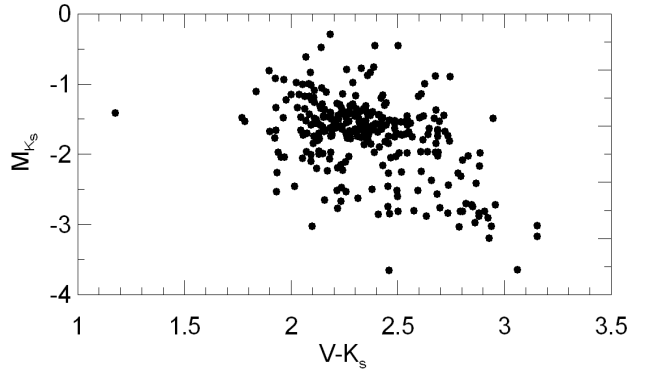


**Fig. 5**  $M_{K_s} \times (V - K_s)$  colour absolute magnitude diagram for 282 RC stars in Alves (2000). The absolute magnitudes are estimated by using the corrected parallaxes.

**Table 2** Mean residuals and the corresponding standard deviations for the data in Laney et al. (2012) and Alves (2000). The statistics in the second and third columns are evaluated by the linear equation in Eq. (4), while those in the fourth and fifth columns correspond to the ones where the  $M_{K_s}$  absolute magnitude is adopted as a constant value,  $M_{K_s} = -1.613$  mag.

Study	Linear Equation		$M_{K_s} = -1.613$	
	$\langle \Delta M_{K_s} \rangle$	$\sigma$	$\langle \Delta M_{K_s} \rangle$	$\sigma$
Laney et al. (2012)	-0.001	0.195	-0.053	0.218
Alves (2000)	+0.209	0.524	+0.133	0.571

**Table 1** Data obtained by combination of the ones in Laney et al. (2012) and the  $V$  apparent magnitudes in *Hipparcos* catalogue. The columns are explained in the text.

(1) ID	(2) Hip	(3) $\pi_0$ (mas)	(4) [ $M/H$ ] (dex)	(5) $V$ (mag)	(6) $K_s$ (mag)	(7) $V - K_s$ (mag)	(8) $M_{K_s}$ (mag)	(1) ID	(2) Hip	(3) $\pi_0$ (mas)	(4) [ $M/H$ ] (dex)	(5) $V$ (mag)	(6) $K_s$ (mag)	(7) $V - K_s$ (mag)	(8) $M_{K_s}$ (mag)	
1	671	10.16	-0.07	5.99	3.653	2.337	-1.312	61	23148	8.84		5.84	3.744	2.096	-1.524	
2	765	22.62		3.88	1.561	2.319	-1.667	62	23430	13.99	0.14	5.01	2.642	2.368	-1.629	
3	814	12.81		5.29	2.968	2.322	-1.494	63	23595	17.99		4.55	1.769	2.781	-1.956	
4	966	8.41	-0.12	6.53	4.151	2.379	-1.225	64	25247	20.73		-0.21	4.13	1.925	2.205	-1.492
5	3137	10.62	0.03	6.00	3.485	2.515	-1.385	65	25532	8.34		6.08	3.802	2.278	-1.592	
6	3455	13.96	-0.06	4.77	2.466	2.304	-1.810	66	26001	14.08		5.34	2.930	2.410	-1.327	
7	3456	9.63	-0.01	5.90	3.295	2.605	-1.787	67	26019	12.67		5.75	3.242	2.508	-1.244	
8	3781	15.40		5.09	2.013	3.077	-2.050	68	26661	6.85		6.77	4.673	2.097	-1.149	
9	4257	7.61	-0.46	6.15	3.910	2.240	-1.683	69	27280	10.95		5.78	3.710	2.070	-1.093	
10	4587	10.20	-0.23	5.62	3.381	2.239	-1.576	70	27369	7.21		6.54	4.127	2.413	-1.583	
11	5170	8.52	0.02	6.12	3.689	2.431	-1.659	71	27530	18.45		4.50	2.036	2.464	-1.634	
12	5364	26.32	0.09	3.46	0.875	2.585	-2.023	72	27549	9.10		5.79	3.749	2.041	-1.456	
13	5485	8.43	0.08	6.40	4.065	2.335	-1.306	73	27621	12.72		5.16	2.921	2.239	-1.556	
14	6537	28.66	-0.10	3.60	1.178	2.422	-1.536	74	27628	37.41		3.12	0.560	2.560	-1.575	
15	6592	13.84	-0.18	5.42	3.019	2.401	-1.276	75	27654	28.68		-0.63	3.76	1.314	2.446	-1.398
16	6732	11.69	0.00	5.50	2.998	2.502	-1.663	76	27766	10.13		5.62	3.223	2.397	-1.749	
17	6868	8.73		6.22	3.760	2.460	-1.535	77	28011	10.31		5.87	3.315	2.555	-1.619	
18	7083	22.95	-0.28	3.93	1.638	2.292	-1.558	78	28085	11.28		5.95	3.376	2.574	-1.363	
19	7271	8.02	-0.34	6.11	3.839	2.271	-1.640	79	28139	10.57		5.89	3.419	2.471	-1.460	
20	7643	9.82	-0.10	5.94	3.557	2.383	-1.482	80	28988	8.87		6.48	3.915	2.565	-1.345	
21	7879	8.28		6.33	4.132	2.198	-1.278	81	29233	6.85		6.27	3.822	2.448	-2.000	
22	7955	15.18	-0.20	5.25	2.845	2.405	-1.248	82	29294	9.89		5.72	3.282	2.438	-1.742	
23	8404	10.16		5.91	3.666	2.244	-1.300	83	29575	10.61		5.83	3.704	2.126	-1.167	
24	8833	18.21	0.01	4.61	2.469	2.141	-1.230	84	29807	17.87		4.37	2.181	2.189	-1.558	
25	8928	14.91		4.68	2.486	2.194	-1.647	85	29842	10.92		5.54	3.004	2.536	-1.805	
26	9440	11.08	-0.47	5.34	3.176	2.164	-1.601	86	30565	12.08		5.37	3.103	2.267	-1.486	
27	9572	9.10		5.87	3.695	2.175	-1.510	87	30728	10.59		5.55	3.188	2.362	-1.688	
28	10234	8.40		5.94	3.666	2.274	-1.712	88	31061	7.44		6.68	4.383	2.297	-1.259	
29	11095	10.28		5.99	3.533	2.457	-1.407	89	31977	7.55		6.50	4.028	2.472	-1.583	
30	11381	11.89		5.89	3.199	2.691	-1.425	90	32222	7.31		6.36	4.101	2.259	-1.579	
31	11524	9.09	0.04	6.11	3.652	2.458	-1.555	91	34142	9.44		6.09	3.410	2.680	-1.715	
32	11757	11.49		5.27	2.996	2.274	-1.702	92	34270	6.18		6.47	4.119	2.351	-1.926	
33	11791	12.28	-0.05	5.36	3.067	2.293	-1.487	93	34440	10.11		5.47	3.114	2.356	-1.862	
34	12148	11.02		5.81	3.352	2.458	-1.437	94	35044	12.00		5.58	2.823	2.757	-1.781	
35	12486	21.65	-0.33	4.11	1.706	2.404	-1.617	95	36444	9.06		5.87	3.545	2.325	-1.669	
36	12608	7.91	0.01	5.99	3.917	2.073	-1.592	96	36732	11.96		5.64	3.126	2.514	-1.486	
37	13147	18.89	-0.34	4.45	2.139	2.311	-1.480	97	37202	8.03		6.20	3.867	2.333	-1.609	
38	13288	17.45	-0.04	4.76	2.668	2.092	-1.123	98	37447	22.07	0.01	3.94	1.614	2.326	-1.667	
39	13701	23.89	-0.11	3.89	1.372	2.518	-1.737	99	37504	23.13		3.93	1.565	2.365	-1.614	
40	14060	10.07		5.75	3.353	2.397	-1.632	100	37590	10.33		5.64	3.412	2.228	-1.518	
41	14168	12.32		5.32	3.168	2.152	-1.379	101	37664	15.03		5.12	2.654	2.466	-1.461	
42	14838	19.22	0.09	4.35	2.052	2.298	-1.529	102	37901	12.18		5.49	2.387	3.103	-2.185	
43	16290	10.17		5.68	3.550	2.130	-1.413	103	38211	12.81		5.17	2.246	2.924	-2.216	
44	17086	7.49		6.22	3.880	2.340	-1.748	104	38375	10.67		5.62	3.466	2.154	-1.393	
45	17351	17.70		4.59	1.995	2.595	-1.765	105	40084	18.46	0.09	4.72	2.585	2.135	-1.084	
46	17595	9.73		5.91	3.634	2.276	-1.425	106	40107	11.22		5.36	3.279	2.081	-1.471	
47	17738	12.13	-0.31	5.52	3.229	2.291	-1.351	107	40888	21.00		4.34	1.764	2.576	-1.625	
48	18199	9.29	0.13	5.93	3.182	2.748	-1.978	108	40990	10.50		5.71	3.275	2.435	-1.619	
49	18401	9.66	-0.10	6.14	3.645	2.495	-1.430	109	41191	13.18		5.67	3.164	2.506	-1.236	
50	18554	5.62		6.94	4.551	2.389	-1.700	110	41312	30.33		3.77	1.210	2.560	-1.381	
51	18635	6.24		6.83	4.307	2.523	-1.717	111	41321	8.90		5.95	3.782	2.168	-1.471	
52	19511	11.40		5.70	3.341	2.359	-1.375	112	41395	11.86		5.52	2.823	2.697	-1.806	
53	19747	28.36	-0.02	3.85	1.337	2.513	-1.399	113	41907	8.25		6.11	3.882	2.228	-1.536	
54	19805	12.41		5.45	2.926	2.524	-1.605	114	41939	7.87		6.36	4.172	2.188	-1.348	
55	20161	12.94		5.33	2.838	2.492	-1.603	115	42134	14.69		4.84	2.559	2.281	-1.606	
56	20825	9.11		5.74	3.459	2.281	-1.744	116	42662	15.40		4.87	2.471	2.399	-1.591	
57	20877	17.47	-0.05	4.96	2.338	2.622	-1.450	117	42717	10.03		6.26	3.532	2.728	-1.462	
58	21594	29.69	0.01	3.86	1.328	2.532	-1.309	118	42911	24.98	-0.01	3.94	1.491	2.449	-1.521	
59	22081	6.72		6.46	4.058	2.402	-1.805	119	42915	8.40		6.66	3.967	2.693	-1.411	
60	22479	13.83	0.05	5.03	2.791	2.239	-1.505	120	43026	10.80		5.70	3.239	2.461	-1.594	

**Table 1** Continued

(1) ID	(2) Hip	(3) $\pi$ (mas)	(4) [M/H] (dex)	(5) $V$ (mag)	(6) $K_s$ (mag)	(7) $V - K_s$ (mag)	(8) $M_{K_s}$ (mag)	(1) ID	(2) Hip	(3) $\pi$ (mas)	(4) [M/H] (dex)	(5) $V$ (mag)	(6) $K_s$ (mag)	(7) $V - K_s$ (mag)	(8) $M_{K_s}$ (mag)
121	43580	9.62		6.12	3.516	2.604	-1.568	173	70306	20.72		4.78	1.776	3.004	-1.642
122	45166	8.39		6.13	3.618	2.512	-1.763	174	72471	12.10		6.21	3.624	2.586	-0.962
123	45439	14.52		4.92	2.457	2.463	-1.733	175	73620	16.69	-0.10	4.39	1.952	2.438	-1.935
124	45542	6.13		7.11	4.908	2.202	-1.155	176	74395	27.80		3.41	1.293	2.117	-1.487
125	45796	7.34		6.70	3.887	2.813	-1.784	177	75119	13.63	-0.02	5.35	2.607	2.743	-1.720
126	45811	14.66	0.05	4.80	2.709	2.091	-1.460	178	75127	10.79	0.06	5.54	3.246	2.294	-1.589
127	45856	13.96		4.79	2.564	2.226	-1.712	179	76333	19.99	-0.30	3.91	1.506	2.404	-1.990
128	46026	16.98	-0.06	4.71	2.597	2.113	-1.254	180	76532	11.87	0.24	5.79	3.344	2.446	-1.284
129	46371	20.83	0.11	4.72	2.145	2.575	-1.262	181	76664	10.09	-0.04	6.19	3.530	2.660	-1.450
130	46736	11.69		5.86	2.990	2.870	-1.671	182	77070	44.10	0.16	2.63	0.097	2.533	-1.681
131	46771	15.13	-0.05	4.99	2.581	2.409	-1.520	183	77578	11.93	-0.18	5.21	2.838	2.372	-1.779
132	46869	7.99		6.12	3.872	2.248	-1.615	184	77853	19.36	-0.21	4.13	1.747	2.383	-1.819
133	47172	8.78		6.18	3.774	2.406	-1.508	185	78639	14.86	-0.05	4.65	2.552	2.098	-1.588
134	47205	13.28		5.00	2.590	2.410	-1.794	186	78650	15.71	-0.01	4.96	2.122	2.838	-1.897
135	48119	9.84		6.05	3.914	2.136	-1.121	187	78685	9.04	0.01	6.07	3.921	2.149	-1.298
136	48806	6.86		6.59	4.076	2.514	-1.742	188	79666	9.38	0.13	5.72	3.248	2.472	-1.891
137	49418	7.13		6.27	3.790	2.480	-1.944	189	79882	30.64	-0.10	3.23	1.010	2.220	-1.558
138	49477	7.61		6.50	4.233	2.267	-1.360	190	80000	25.33	0.23	4.01	1.628	2.382	-1.354
139	49841	28.98	0.17	3.61	1.391	2.219	-1.298	191	80343	16.35	-0.13	4.48	2.163	2.317	-1.770
140	50234	9.31		6.17	3.765	2.405	-1.391	192	81852	20.78	-0.05	4.23	1.812	2.418	-1.600
141	50799	16.00		4.82	2.360	2.460	-1.619	193	82396	51.19	-0.05	2.29	-0.285	2.575	-1.739
142	51077	10.20		6.13	3.604	2.526	-1.353	194	83000	35.66	0.09	3.19	0.656	2.534	-1.583
143	52085	15.49	-0.10	4.91	2.788	2.122	-1.262	195	86170	19.67	-0.25	4.26	1.696	2.564	-1.835
144	52660	10.04		6.38	3.854	2.526	-1.137	196	86391	8.85	0.14	6.25	3.892	2.358	-1.373
145	52689	11.35		5.49	3.385	2.105	-1.340	197	86742	39.85	0.14	2.76	0.219	2.541	-1.779
146	52948	9.57		5.85	3.397	2.453	-1.698	198	88635	33.67	-0.24	2.98	0.644	2.336	-1.720
147	53273	10.43		5.45	3.273	2.177	-1.635	199	89153	12.74	-0.06	4.96	2.560	2.400	-1.914
148	53394	10.70		5.93	3.407	2.523	-1.446	200	89587	9.67	-0.60	5.99	3.789	2.201	-1.284
149	53502	17.16		4.60	2.296	2.304	-1.532	201	90496	41.72	-0.07	2.82	0.382	2.438	-1.516
150	54264	8.03		6.28	4.033	2.247	-1.444	202	90568	25.84	-0.20	4.10	1.708	2.392	-1.230
151	54291	8.54		6.31	3.765	2.545	-1.577	203	93498	12.66	0.36	5.63	2.956	2.674	-1.532
152	55249	11.08		5.90	3.489	2.411	-1.288	204	93683	22.96	-0.01	3.76	1.455	2.305	-1.740
153	56287	10.64		5.89	3.376	2.514	-1.490	205	94005	18.27	0.01	4.57	2.137	2.433	-1.554
154	56343	25.16	0.08	3.54	1.417	2.123	-1.579	206	98575	9.29	0.04	6.01	3.798	2.212	-1.362
155	56656	13.95		5.14	2.631	2.509	-1.646	207	98624	13.80	0.11	5.32	2.621	2.699	-1.679
156	56996	9.05		6.32	3.705	2.615	-1.512	208	99570	9.99	0.22	6.20	3.512	2.688	-1.490
157	57791	10.94		5.62	3.182	2.438	-1.623	209	101772	33.17	-0.13	3.11	0.811	2.299	-1.585
158	58697	8.79		6.05	3.116	2.934	-2.164	210	103738	14.24	-0.11	4.67	2.596	2.074	-1.637
159	58706	7.53		6.41	3.718	2.692	-1.898	211	105425	9.08		6.40	3.521	2.879	-1.688
160	58948	19.98	-0.39	4.12	1.869	2.251	-1.628	212	106039	19.06	-0.09	4.50	2.426	2.074	-1.173
161	59785	8.12		6.24	3.855	2.385	-1.597	213	111600	9.12	-0.03	5.82	3.319	2.501	-1.881
162	61181	9.38		5.88	3.452	2.428	-1.687	214	112127	9.21		6.06	3.851	2.209	-1.327
163	62012	17.11		4.66	2.249	2.411	-1.585	215	112203	14.16	-0.20	4.84	2.493	2.347	-1.752
164	63608	29.76	0.27	2.85	0.786	2.064	-1.846	216	113246	21.16	-0.20	4.20	1.951	2.249	-1.421
165	65468	14.75		5.04	2.560	2.480	-1.596	217	114119	15.08	-0.02	4.48	2.319	2.161	-1.789
166	66936	13.68	0.11	5.35	2.849	2.501	-1.470	218	114855	21.77	-0.01	4.24	1.746	2.494	-1.565
167	67494	13.35	0.09	4.96	2.597	2.363	-1.776	219	114971	23.64	-0.52	3.70	1.441	2.259	-1.691
168	68079	10.25		5.82	3.269	2.551	-1.677	220	115102	17.90	-0.08	4.41	1.886	2.524	-1.849
169	68933	55.45		2.06	-0.273	2.333	-1.554	221	115620	11.23	0.08	5.60	3.224	2.376	-1.524
170	69191	17.88		4.74	2.601	2.139	-1.137	222	115830	21.96	0.03	4.27	1.889	2.381	-1.403
171	69612	12.31	-0.14	5.29	2.946	2.344	-1.603	223	115919	18.65	0.07	4.54	2.425	2.115	-1.222
172	70027	17.44	0.12	4.84	2.141	2.699	-1.651	224	116853	9.34	0.10	5.89	3.710	2.180	-1.438

**Table 3** Data taken from Alves (2000). The columns are explained in the text.

(1)	(2)	(3)	(4)	(5)	(6)	(7)	(8)	(9)	(1)	(2)	(3)	(4)	(5)	(6)	(7)	(8)	(9)
ID	Hip	$\pi_0$ (mas)	[M/H] (dex)	V (mag)	$K_s$ (mag)	$V - K_s$ (mag)	$M_{K_s}$ (mag)	Quality	ID	Hip	$\pi_0$ (mas)	[M/H] (dex)	V (mag)	$K_s$ (mag)	$V - K_s$ (mag)	$M_{K_s}$ (mag)	Quality
1	443	25.28	-0.31	4.613	1.989	2.624	-0.997	DCD	76	30277	13.86	-0.31	3.852	1.836	2.016	-2.455	DDD
2	476	8.71	-0.22	5.550	3.767	1.783	-1.533	DDD	77	32249	11.27	-0.26	4.493	1.861	2.632	-2.879	DCD
3	729	11.40	-0.01	5.570	3.321	2.249	-1.394	DDD	78	33449	18.28	0.05	4.350				DCX
4	873	13.29	-0.02	5.841	3.772	2.069	-0.610	DDD	79	36046	27.09	-0.17	3.777	1.562	2.215	-1.274	DCD
5	1708	9.80	0.00	5.176	3.045	2.131	-1.999	DDD	80	37447	22.06	-0.11	3.942	1.643	2.299	-1.639	DDD
6	2568	12.47	-0.08	5.377	2.950	2.427	-1.571	DCD	81	37740	23.06	-0.16	3.573	1.527	2.046	-1.659	DCD
7	3031	19.90	-0.64	4.342	2.074	2.268	-1.432	DCD	82	37826	96.54	-0.07	1.158	-0.936	2.094	-1.012	DCD
8	3092	30.91	0.04	3.269	0.467	2.802	-2.083	DCC	83	39079	11.85	-0.24	4.930	2.192	2.738	-2.439	DDD
9	3231	9.15	-0.26	5.302	3.231	2.071	-1.962	DCD	84	39424	12.47	0.03	4.942	2.476	2.466	-2.045	DCD
10	3419	33.86	-0.09	2.040	-0.274	2.314	-2.626	CDD	85	40084	18.45	-0.03	4.723	2.670	2.053	-1.000	DDD
11	3455	13.94	-0.16	4.767	2.575	2.192	-1.704	DCC	86	41325	8.21	-0.34	5.130	2.915	2.215	-2.513	DCD
12	4422	16.31	-0.51	4.619	2.468	2.151	-1.470	DCD	87	42483	13.33	-0.49	4.864	2.900	1.964	-1.476	DDD
13	4463	14.18	-0.54	4.402	2.254	2.148	-1.988	DDD	88	42527	12.72	-0.26	4.586	1.734	2.852	-2.744	DCD
14	4587	10.09	-0.37	5.615	3.413	2.202	-1.568	DCC	89	42662	15.39	-0.01	4.868	2.637	2.231	-1.427	DDD
15	4906	17.93	-0.39	4.270	2.121	2.149	-1.611	DDD	90	42911	24.97	-0.13	3.938	1.567	2.371	-1.446	DCC
16	5364	26.32	-0.03	3.465	0.922	2.543	-1.977	DCC	91	43409	15.72	-0.11	4.020	1.140	2.880	-2.878	DCD
17	5586	19.31	-0.04	4.507	2.148	2.359	-1.423	DCD	92	43813	19.50	-0.21	3.106	0.697	2.409	-2.853	DCC
18	6411	15.19	0.03	4.871	2.554	2.317	-1.538	DDD	93	45751	9.55	-0.20	4.773	2.840	1.933	-2.260	DDD
19	6537	28.65	-0.22	3.603	1.289	2.314	-1.425	DCC	94	45811	14.63	-0.07	3.936	2.761	1.175	-1.413	DCD
20	6692	16.71	-0.13	4.718	2.324	2.394	-1.561	DCD	95	46026	16.97	-0.18	4.707	2.707	2.000	-1.145	DDD
21	6732	11.67	-0.12	5.503	3.087	2.416	-1.578	DDD	96	46146	16.19	0.01	4.471	1.688	2.783	-2.266	DCC
22	6999	11.06	-0.16	5.268	3.115	2.153	-1.666	DCD	97	46371	20.46	-0.01	4.719	2.291	2.428	-1.154	DDD
23	7294	15.63	-0.36	4.675	2.311	2.364	-1.719	CDC	98	46771	15.10	-0.17	4.989	2.716	2.273	-1.389	DDD
24	7607	18.40	0.00	3.586	0.649	2.937	-3.027	DBC	99	46952	17.62	-0.15	4.538				DDX
25	7719	12.94	-0.21	5.015	2.969	2.046	-1.471	DCD	100	47029	15.13	-0.18	4.806	2.629	2.177	-1.472	DCD
26	7955	15.05	-0.29	5.253	2.950	2.303	-1.162	DCD	101	48455	26.28	0.17	3.878	1.364	2.514	-1.538	DCD
27	8198	11.51	-0.11	4.257	2.025	2.232	-2.670	DDD	102	48559	9.49	-0.03	4.866	2.078	2.788	-3.036	DDD
28	8833	18.08	-0.11	4.606	2.541	2.065	-1.173	DDD	103	49841	28.88	0.05	3.610	1.525	2.085	-1.172	DDD
29	9440	11.05	-0.59	5.343	3.218	2.125	-1.565	DDD	104	51233	21.14	0.00	4.196	2.061	2.135	-1.313	CDC
30	9763	8.12	-0.10	5.218	2.982	2.236	-2.470	DCD	105	51775	12.24	-0.25	5.069	2.977	2.092	-1.584	DDD
31	9884	49.55	-0.25	2.012	-0.783	2.795	-2.308	DCC	106	52085	15.41	-0.22	4.910	2.800	2.110	-1.261	DDD
32	10642	9.73	-0.10	5.075	3.320	2.187	-1.739	DCD	107	52353	14.36	0.06	5.119	2.234	2.885	-1.980	CDC
33	11791	12.21	-0.17	5.364	3.207	2.157	-1.359	DCD	108	52943	22.68	-0.30	3.109	0.248	2.861	-2.974	DDD
34	13061	19.00	-0.02	4.524	2.099	2.425	-1.507	DCD	109	53229	34.37	-0.20	3.789	1.530	2.259	-0.789	FCF
35	13147	18.88	-0.47	4.449	2.098	2.351	-1.522	DCD	110	53426	13.75	-0.26	5.024	2.334	2.690	-1.974	DDD
36	13288	17.44	-0.17	4.758	2.483	2.275	-1.309	CCD	111	53740	20.48	-0.22	4.080	1.733	2.347	-1.710	DDD
37	13701	23.88	-0.23	3.895	1.471	2.424	-1.639	DDD	112	53807	9.03	-0.28	4.838	2.377	2.461	-2.845	DDD
38	14382	15.43	-0.17	4.774	2.398	2.376	-1.660	DCD	113	54539	22.57	-0.13	3.003	0.429	2.574	-2.803	CDC
39	14668	28.92	0.04	3.786	1.242	2.544	-1.452	DBC	114	56343	25.16	-0.04	3.540	1.471	2.069	-1.525	DDD
40	14817	11.30	-0.10	4.615	2.235	2.380	-2.500	DCD	115	56647	17.96	-0.34	4.304	2.184	2.120	-1.544	DDD
41	14838	19.21	-0.03	4.354	2.169	2.185	-1.413	DCD	116	57283	9.09	-0.11	4.715	2.558	2.157	-2.649	DCD
42	15382	12.33	-0.07	4.864	2.741	2.123	-1.804	DDD	117	57399	17.75	-0.44	3.686	0.988	2.698	-2.766	DCC
43	15383	14.70	-0.10	5.624	2.678	2.946	-1.485	CCD	118	58948	19.97	-0.51	4.123	2.014	2.109	-1.484	DDD
44	15861	15.65	0.00	5.498	2.888	2.610	-1.139	DDD	119	59856	10.25	-0.29	4.987	2.106	2.881	-2.840	DCD
45	15900	10.93	-0.15	3.610	1.152	2.458	-3.655	DCC	120	60172	10.57	-0.48	4.970	2.065	2.905	-2.815	DDD
46	16780	8.55	-0.30	5.563	3.663	1.900	-1.677	DDC	121	60646	12.45	-0.11	5.014	2.856	2.158	-1.668	DDD
47	17738	12.10	-0.43	5.523	3.294	2.229	-1.292	DDD	122	61359	22.38	-0.11	2.651	0.719	1.932	-2.532	DDD
48	19038	17.42	0.01	4.361	2.033	2.328	-1.762	DDD	123	63608	29.76	0.15	2.849	0.664	2.185	-1.968	DDD
49	19388	11.44	-0.02	5.508	3.170	2.338	-1.538	DDD	124	64078	10.59	-0.04	5.149	2.720	2.429	-2.156	DDD
50	19483	9.22	-0.10	5.445	3.516	1.929	-1.660	DCD	125	64166	14.02	-0.19	4.942	2.735	2.207	-1.531	DDD
51	20205	20.17	-0.02	3.649	1.518	2.131	-1.958	DCC	126	64803	12.64	-0.15	5.095	2.975	2.120	-1.516	DDD
52	20266	10.16	-0.18	5.256	3.486	1.770	-1.480	DDD	127	64962	24.37	-0.12	2.993	1.024	1.969	-2.042	DDD
53	20455	20.90	0.00	3.771	1.643	2.128	-1.756	DCD	128	65535	15.95	-0.25	5.114	2.513	2.601	-1.473	DCD
54	20877	17.43	-0.17	4.964	2.344	2.620	-1.450	DDD	129	65639	11.62	0.02	4.757	2.524	2.233	-2.150	DDD
55	20885	21.12	0.04	3.836	1.644	2.192	-1.733	DCD	130	66098	13.84	-0.40	5.210	3.105	2.105	-1.189	DDD
56	20889	22.23	0.04	3.525	1.422	2.103	-1.843	DDD	131	66936	13.49	-0.01	5.352	2.793	2.559	-1.557	DCD
57	21248	25.66	-0.34	4.493	2.122	2.371	-0.832	DCD	132	67494	13.32	-0.03	4.959	2.610	2.349	-1.767	DCC
58	21393	15.24	-0.09	3.808	1.552	2.256	-2.533	DDD	133	68895	32.30	-0.16	3.247	0.753	2.494	-1.701	DDD
59	21594	29.67	-0.11	3.864	1.441	2.423	-1.197	DDD	134	69415	14.96	-0.14	5.075	2.388	2.687	-1.737	DDD
60	21685	16.60	-0.24	5.457	3.127	2.330	-0.772	DDD	135	69612	12.20	-0.26	5.294	2.949	2.345	-1.619	DDD
61	22479	13.80	-0.07	5.026	2.803	2.223	-1.498	DCD	136	69879	13.93	-0.13	4.796	2.384	2.412	-1.896	DDD
62	22957	17.53	-0.26	4.063	1.407	2.656	-2.374	DCC	137	70012	12.44	-0.22	5.138	2.834	2.304	-1.692	DDD
63	23430	1															

**Table 3** Continued

(1) ID	(2) Hip	(3) $\pi_0$ (mas)	(4) [M/H] (dex)	(5) V (mag)	(6) $K_s$ (mag)	(7) $V - K_s$ (mag)	(8) $M_{K_s}$ (mag)	(9) Quality	(1) ID	(2) Hip	(3) $\pi_0$ (mas)	(4) [M/H] (dex)	(5) V (mag)	(6) $K_s$ (mag)	(7) $V - K_s$ (mag)	(8) $M_{K_s}$ (mag)	(9) Quality
151	75458	32.23	0.03	3.290	0.671	2.619	-1.788	DBC	218	97433	22.02	-0.47	3.841	1.732	2.109	-1.554	DCD
152	76133	11.58	-0.13	5.497	2.929	2.568	-1.752	DCD	219	97938	17.75	-0.32	4.715	2.171	2.544	-1.583	DCD
153	76333	19.98	-0.42	3.914	1.524	2.390	-1.973	DDD	220	98110	24.17	-0.09	3.886	1.371	2.515	-1.713	DCD
154	76425	14.08	-0.17	5.264	2.975	2.289	-1.282	DCD	221	98353	10.38	-0.38	4.837	2.718	2.119	-2.201	DCD
155	76534	19.21	-0.55	5.245	3.103	2.142	-0.479	DCD	222	98842	11.20	-0.63	4.991	2.034	2.957	-2.720	DDD
156	76705	14.83	-0.34	4.663	2.290	2.373	-1.854	DDD	223	98920	20.31	-0.03	5.094	2.708	2.386	-0.753	DCD
157	77070	44.10	0.03	2.634	0.150	2.484	-1.628	CDD	224	98962	18.97	0.12	5.399	2.723	2.676	-0.887	DDD
158	77512	19.17	-0.32	4.594	2.668	1.926	-0.919	CCD	225	100064	30.82	-0.18	3.576	1.466	2.110	-1.090	DDD
159	77578	11.90	-0.28	5.207	2.929	2.278	-1.693	DDD	226	100437	7.96	0.00	5.577	2.984	2.593	-2.511	CDD
160	77853	19.36	-0.31	4.127	1.767	2.360	-1.798	DDD	227	101101	16.29	0.03	4.913	2.504	2.409	-1.436	DDD
161	78132	13.46	0.06	5.536	3.091	2.445	-1.264	DDD	228	101936	13.87	-0.12	5.154	2.710	2.444	-1.580	CCD
162	78159	14.72	-0.32	4.142	1.349	2.793	-2.811	DCC	229	102014	13.74	-0.02	5.474	2.778	2.696	-1.532	DDD
163	78481	12.76	-0.31	5.102	2.869	2.233	-1.602	DCC	230	102453	16.21	-0.24	4.219	1.701	2.518	-2.250	DCC
164	78650	15.69	-0.14	4.956	2.213	2.743	-1.809	DDD	231	102488	44.86	-0.27	2.479	-0.007	2.486	-1.748	DCC
165	79119	27.73	-0.20	4.730	2.338	2.392	-0.447	CCC	232	102532	25.55	0.13	4.275	1.595	2.680	-1.368	DDD
166	79302	10.21	-0.36	5.091	1.937	3.154	-3.018	CDC	233	103004	17.20	-0.23	4.559	2.722	1.837	-1.100	DCD
167	79882	30.63	-0.25	3.230	1.146	2.084	-1.423	DDD	234	103519	12.58	0.00	5.553	3.529	2.024	-0.973	DDD
168	80181	17.77	-0.08	4.857	2.615	2.242	-1.137	DCC	235	103738	14.22	-0.23	4.670	2.541	2.129	-1.695	DCC
169	80331	35.42	-0.21	2.732	0.579	2.153	-1.675	DCC	236	104174	9.92	-0.01	5.204	2.747	2.457	-2.270	DCD
170	80894	13.37	0.08	4.286	2.333	1.953	-2.036	DDD	237	104459	20.46	-0.15	4.498	2.334	2.164	-1.111	DCD
171	81437	11.98	-0.12	5.282	2.644	2.638	-1.964	CCC	238	104732	22.77	-0.11	3.214	1.160	2.054	-2.053	CCC
172	81833	30.02	-0.37	3.480	1.333	2.147	-1.280	DCD	239	105411	12.03	-0.24	5.578	3.229	2.349	-1.370	DCD
173	82396	51.19	-0.17	2.288	-0.392	2.680	-1.846	CCD	240	105502	20.92	-0.14	4.081	1.752	2.329	-1.645	DCC
174	82764	12.03	-0.26	5.386	3.128	2.258	-1.471	DDD	241	105515	16.56	-0.23	4.279	2.206	2.073	-1.699	DDD
175	83000	35.66	-0.03	3.188	0.728	2.460	-1.511	DCC	242	106039	19.04	-0.28	4.498	2.263	2.235	-1.339	DDD
176	84514	15.77	-0.03	4.716	2.040	2.676	-1.971	DCC	243	106481	26.39	-0.31	3.982	1.901	2.081	-0.992	DDD
177	85803	15.45	-0.20	5.073	2.426	2.647	-1.629	DDD	244	106551	14.04	-0.08	4.869	2.595	2.274	-1.668	DCD
178	86742	39.85	0.02	2.758	0.437	2.321	-1.561	DCC	245	106944	14.37	-0.17	5.100	2.826	2.274	-1.387	DDD
179	87194	15.37	-0.03	5.093	2.405	2.688	-1.662	CCC	246	107119	17.84	0.04	4.552	1.722	2.830	-2.021	CBC
180	87563	9.17	-0.12	5.174	2.021	3.153	-3.167	CCC	247	107128	14.12	-0.01	5.240	2.901	2.339	-1.350	DDD
181	87585	28.98	-0.09	3.731	1.045	2.686	-1.645	DCC	248	107188	11.06	-0.20	4.720	2.549	2.171	-2.232	DCD
182	87847	8.10	-0.16	5.441	2.946	2.495	-2.512	DDD	249	108868	10.70	-0.11	5.550	3.521	2.029	-1.332	DDD
183	87933	23.84	-0.10	3.702	1.491	2.211	-1.622	DCC	250	109786	13.82	-0.13	5.330	3.364	1.966	-0.933	DDF
184	88048	21.63	0.02	3.317	1.225	2.092	-2.100	DDD	251	110003	17.39	0.01	4.167	2.061	2.106	-1.738	DDD
185	88635	33.67	-0.36	2.984	0.545	2.439	-1.819	DDD	252	110529	12.39	-0.07	5.526	3.143	2.383	-1.392	DCD
186	88765	11.93	-0.10	4.645	2.426	2.219	-2.191	DCC	253	110538	19.18	-0.39	4.418	1.880	2.538	-1.706	DCD
187	88788	7.76	-0.06	4.996	2.778	2.218	-2.773	DDD	254	110882	21.97	-0.37	4.777	2.420	2.357	-0.871	DDD
188	89008	8.24	-0.14	5.571	3.648	1.923	-1.772	DCC	255	111710	15.24	0.14	5.038	2.610	2.428	-1.475	DCC
189	89065	8.02	-0.03	5.501	2.577	2.924	-2.902	DCC	256	112067	11.72	-0.09	5.925	3.210	2.715	-1.445	CCD
190	89153	12.71	-0.18	4.957	2.615	2.342	-1.864	DDD	257	112529	12.80	-0.43	5.243	3.061	2.182	-1.403	DDD
191	89772	21.35	0.05	5.406	2.904	2.502	-0.449	DCC	258	112722	28.29	-0.12	3.497	1.276	2.221	-1.466	DCD
192	89826	12.95	-0.09	4.335	1.838	2.497	-2.601	DCC	259	112731	8.18	-0.53	5.428	2.625	2.803	-2.811	DCD
193	89918	12.49	-0.21	4.846	2.791	2.055	-1.726	DDD	260	112748	30.73	-0.16	3.512	1.181	2.331	-1.381	DCC
194	89962	53.93	-0.42	3.234	1.050	2.184	-0.291	DDD	261	113084	10.66	-0.02	5.818	3.514	2.304	-1.347	DDD
195	90135	15.51	-0.17	4.663	2.545	2.118	-1.502	DCC	262	113184	11.85	0.04	5.723	3.826	1.897	-0.805	DDD
196	90139	27.40	-0.16	3.854	1.311	2.543	-1.500	DCC	263	113246	21.14	-0.31	4.200	1.881	2.319	-1.493	DDD
197	90344	10.34	-0.44	4.820	2.085	2.735	-2.842	DCC	264	113521	10.89	-0.04	5.428	2.972	2.456	-1.843	DCD
198	90496	41.72	-0.20	2.817	0.332	2.485	-1.566	DCC	265	113864	7.87	0.07	5.252	2.325	2.927	-3.195	CCD
199	90642	14.15	-0.08	5.381	2.944	2.437	-1.302	CCC	266	113919	18.45	-0.20	4.640	2.154	2.486	-1.516	DCD
200	91105	9.88	-0.07	5.116	3.022	2.094	-2.004	DCC	267	114119	14.94	-0.14	4.483	2.351	2.132	-1.777	DDD
201	92088	12.78	-0.12	4.833	2.222	2.611	-2.245	DCC	268	114222	12.94	0.01	4.406	2.468	1.938	-1.972	DCD
202	92689	6.79	-0.14	4.917	2.819	2.098	-3.022	DDD	269	114641	9.40	-0.33	5.848	3.392	2.456	-1.742	DDD
203	92782	9.39	-0.12	4.822	2.321	2.501	-2.816	DDD	270	114855	21.75	-0.14	4.239	1.597	2.642	-1.716	DCD
204	92872	11.02	-0.26	5.584	3.064	2.520	-1.725	DCC	271	114971	23.64	-0.61	3.703	1.393	2.310	-1.740	DDD
205	93026	16.10	-0.11	4.829	2.533	2.296	-1.433	DCC	272	115088	16.03	-0.07	4.749	2.528	2.221	-1.447	DCD
206	93244	20.96	0.00	4.024	1.786	2.238	-1.607	DCC	273	115102	17.89	-0.22	4.405	1.718	2.687	-2.019	DCD
207	93429	22.65	-0.19	4.017	1.636	2.381	-1.589	DDD	274	115227	7.45	-0.63	5.052	1.993	3.059	-3.646	DCD
208	93683	22.95	-0.11	3.755	1.573	2.182	-1.623	DDD	275	115438	19.95	-0.40	3.960	1.468	2.492	-2.032	DDD
209	93864	26.71	-0.17	3.324	0.458	2.866	-2.409	DDD	276	115830	21.95	-0.12	4.273	1.859	2.414	-1.434	DCD
210	94376	33.48	-0.27	3.072	0.883	2.189	-1.493	DCC	277	115919	18.52	-0.03	4.537	2.442	2.095	-1.220	DDD
211	94648	22.24	0.12	4.445	1.775	2.670	-1.489	DCC	278	116076	12.61	-0.36	5.215	2.331	2.884	-2.165	CCD
212	94779	26.27	-0.08	3.795	1.757	2.038											